Published in final edited form as:

Ann Nucl Med. 2018 January ; 32(1): 69–74. doi:10.1007/s12149-017-1216-x.

Low Levels of PSMA Expression Limit the Utility of ^{18}F-DCFPyL PET/CT for Imaging Urothelial Carcinoma

Scott P. Campbell[1], **Alexander S. Baras**[2], **Mark W. Ball**[1], **Max Kates**[1], **Noah M. Hahn**[3], **Trinity J. Bivalacqua**[1,3], **Michael H. Johnson**[1], **Martin G. Pomper**[1,3,4], **Mohamad E. Allaf**[1,3], **Steven P. Rowe**[1,4], and **Michael A. Gorin**[1,2,3,4]

[1]The James Buchanan Brady Urological Institute and Department of Urology, Johns Hopkins University School of Medicine, Baltimore, MD, USA

[2]Department of Pathology, Johns Hopkins University School of Medicine, Baltimore, MD, USA

[3]Department of Oncology, Sidney Kimmel Comprehensive Cancer Center, Johns Hopkins University School of Medicine, Baltimore, MD, USA

[4]The Russell H. Morgan Department of Radiology and Radiological Science, Johns Hopkins University School of Medicine, Baltimore, MD, USA

Abstract

Objective—To explore the clinical utility of PSMA-targeted ^{18}F-DCFPyL PET/CT in patients with metastatic urothelial carcinoma.

Methods—Three patients with metastatic urothelial were imaged with ^{18}F-DCFPyL PET/CT. All lesions with perceptible radiotracer uptake above background were considered positive. Maximum standardized uptake values were recorded for each detected lesion and findings on ^{18}F-DCFPyL PET/CT were compared to those on conventional imaging studies. To further explore PSMA as a molecular target of urothelial carcinoma, RNA-sequencing data from The Cancer Genome Atlas was used to compare the relative expression of PSMA among cases of bladder cancer, prostate cancer, and clear cell renal cell carcinoma. Additionally, immunohistochemical staining for PSMA expression was performed on a biopsy specimen from one of the imaged patients.

Results—^{18}F-DCFPyL PET/CT allowed for the detection of sites of urothelial carcinoma, albeit with low levels of radiotracer uptake. Analysis of RNA-sequencing data revealed that bladder cancer had significantly lower levels of PSMA expression than both prostate cancer and clear cell renal cell carcinoma. Consistent with this observation, immunohistochemical staining of tissue from one of the imaged patients demonstrated a low level of neovascularization and nearly absent PSMA expression.

Conclusion—The relatively scant expression of PSMA by urothelial cancer likely limits the utility of PSMA-targeted PET imaging of this malignancy. Future research efforts should focus on the development of other molecularly targeted imaging agents for urothelial carcinoma.

Corresponding Author: Michael A. Gorin, M.D., 600 North Wolfe Street, Park 213, Baltimore, MD 21287, gorin1@jhmi.edu, Phone: (410) 502-7710, Fax: (410) 502-7711.

Keywords

prostate-specific membrane antigen; PSMA; ^{18}F-DCFPyL PET/CT; urothelial carcinoma; bladder cancer; transitional cell carcinoma

Introduction

At the present time, the mainstays of imaging for urothelial carcinoma of bladder and upper urinary tract are computed tomography (CT) and magnetic resonance imaging (MRI) [1]. These imaging modalities, however, are limited in their ability to detect sub-centimeter sites of metastatic disease. This is evident by the fact that upwards of 20% of patients with clinically localized urothelial carcinoma of the bladder will be found to have positive lymph nodes at the time of radical cystectomy [2]. As an adjunct to CT and MRI, positron emission tomography (PET) using the metabolic radiotracer 2-deoxy-2-[^{18}F]fluoro-D-glucose (^{18}F-FDG) has been explored in patients with urothelial carcinoma; however, this test has shown only modest improvements in the ability to detect small volume sites of disease [3-6].

Owing to the limitations of currently available modalities for imaging urothelial carcinoma, there has been growing interest in the development of molecularly targeted imaging agents for this disease. One molecular target of particular promise is the type II glycoprotein known as prostate-specific membrane antigen (PSMA), which despite the specificity implied by its name is highly expressed in the neovasculature of a number of solid malignancies including urothelial carcinoma [7-10]. PSMA-targeted PET imaging has been widely studied in men with prostate cancer (Reviewed in [11]) and more recently has been explored in other malignancies [12-21]. Among these, clear cell renal cell carcinoma is the most well studied and initial reports suggest that PET/CT utilizing PSMA-targeted radiotracers may detect metastatic lesions with higher sensitivity than CT, MRI, and ^{18}F-FDG PET/CT [12-16]. Additionally, PSMA-targeted imaging has been shown to have potential for the detection of other solid malignancies including cancers of the bone [17], brain [18], breast [19], gastrointestinal tract [20], liver [21] and thyroid [22].

Early studies utilizing the radiolabeled J591 antibody have demonstrated initial feasibility of imaging urothelial carcinoma using PSMA-targeted agents [23, 24]. More recently, a case report was published on the successful imaging of a patient with metastatic upper tract urothelial carcinoma using the urea-based small molecule inhibitor of PSMA known as ^{68}Ga-PSMA-11 (also known as ^{68}Ga-PSMA-HBED-CC) [25]. While ^{68}Ga-PSMA-11 is the most widely utilized agent for PSMA-targeted PET imaging, a handful of other radiotracers have been developed including ^{18}F-DCFPyL [26-28]. Available data suggests that PET imaging with ^{18}F-DCFPyL may offer improved image quality and lesion detection relative to the ^{68}Ga-PSMA-11 radiotracer [29,30].

Herein, we present data from three patients with metastatic urothelial carcinoma imaged with ^{18}F-DCFPyL PET/CT. Although this imaging test allowed for the detection of sites of urothelial carcinoma, only modest levels of radiotracer uptake were observed. Our findings suggest that PSMA-targeted PET likely does not afford improved sensitivity over conventional modalities for imaging this malignancy.

Patients and Methods

Three patients with metastatic urothelial carcinoma were imaged with ^{18}F-DCFPyL PET/CT as previously described by Rowe *et al.* [12]. Patients were imaged following enrollment in an institutional review board-approved clinical study investigating the utility of this imaging test in patients with non-prostate epithelial malignancies. In brief, 1 hour after intravenous administration of ~9 mCi of the ^{18}F-DCFPyL radiotracer, a PET/CT was acquired from the mid-thigh to the vertex of the skull. In order to decrease bladder activity, patients were asked to void prior to imaging.

Acquired images were reviewed by a single radiologist with extensive experience in interpreting ^{18}F-DCFPyL PET/CT studies (S.P.R.). Any lesion with perceptible radiotracer uptake above background was considered positive. Lean body mass corrected maximum standardized uptake values (SUV_{max},) were recorded for each detected lesion and findings on ^{18}F-DCFPyL PET/CT were compared to those on contemporaneously acquired conventional imaging studies.

To more broadly explore PSMA as a molecular target of urothelial carcinoma, RNA-sequencing data from The Cancer Genome Atlas was used to compare the relative expression of *FOLH1* (the gene that encodes the PSMA protein) among cases of bladder cancer, prostate cancer, and clear cell renal cell carcinoma. RNA-sequencing data were obtained from the Broad Institute Genome Data Analysis Center (http://firebrowse.org) with transcript quantification having already been performed using RNA-Sequencing by Expectation Maximization (RSEM) [31]. Log-transformed normalized RSEM values [32] for each cancer type were compared using the Kruskal-Wallis test. Statistical analysis was performed with Stata 13.1 (StataCorp, College Station, TX). A two-tailed $P < 0.05$ was defined as statistical significance. To further expand upon this analysis, immunohistochemistry was performed on a biopsy specimen from one of the imaged patients (Patient 1) using antibodies against PSMA and the endothelial cell marker CD34. For comparison, tissue from two additional patients, one with prostate cancer and the second with clear cell renal cell carcinoma, were also stained.

Results

The characteristics of the three imaged patients are provided in Table 1.

The first patient had a history of metastatic urothelial carcinoma of the bladder treated with gemcitabine/cisplatin followed by atezolizumab. On surveillance imaging the patient was noted to have a recurrent lesion of the prostatic urethra. This lesion was visible on both pelvic MRI and ^{18}F-FDG PET/CT with an SUV_{max} of 9.0 (Figure 1). This lesion had no discernable uptake above background with ^{18}F-DCFPyL.

The second patient presented with a tumor of the bladder as well as extensive pelvic lymph node involvement. Imaging was performed prior to administration of systemic therapy. Both the bladder mass and adenopathy were visible on contrast-enhanced CT (Figure 2). On ^{18}F-DCFPyL PET/CT, these lesions demonstrated only modest radiotracer uptake with SUV_{max} in the range of 2.0 to 2.5.

The third patient had a history of metastatic urothelial carcinoma of the right renal pelvis treated with nephroureterectomy and gemcitabine/cisplatin. On conventional imaging the patient was noted to have an enlarged aortocaval lymph node measuring 2.2 cm and a 1.2 cm right lower lobe lung metastasis. This patient's lymph node was visible on ^{18}F-FDG PET/CT with an SUV_{max} of 5.7 (Figure 3). This lesion was also identifiable on ^{18}F-DCFPyL PET/CT, albeit with a lower SUV_{max} value of 3.1. The patient's lung lesion was visible with both imaging modalities; however, ^{18}F-FDG PET/CT provided for superior image quality and a higher SUV_{max} relative to ^{18}F-DCFPyL (4.6 versus 1.5).

Comparison of gene expression levels utilizing RNA-sequencing data demonstrated that bladder cancer had significantly lower levels of *FOLH1* gene expression than both prostate cancer and clear cell renal cell carcinoma (Figure 4). Moreover, immunohistochemical staining of the tumor specimen from Patient 1 demonstrated scant neovascularization and almost no detectable PSMA expression (Figure 5). In contrast, staining for PSMA was abundant in the prostate cancer and renal cell carcinoma specimens. In the case of prostate cancer, PSMA expression was present on the epithelial cells of the tumor, whereas in the case of clear cell renal cell carcinoma the expression was restricted to the endothelial cells of the tumor neovasculature.

Discussion

In the presented series of 3 patients, PSMA-targeted PET imaging using the ^{18}F-DCFPyL radiotracer allowed for the detection of foci of urothelial carcinoma across a range of anatomic sites including the bladder, lymph nodes, and lung. The degree of radiotracer uptake, however, was universally low and less than that with ^{18}F-FDG in the 2 patients in whom contemporaneous imaging was available for comparison. As evident by RNA-sequencing data and immunohistochemical staining, the poor performance of ^{18}F-DCFPyL PET/CT for imaging urothelial cancer is likely explained by scant tumor neovascularization and low associated levels of PSMA expression.

A major limitation of this study is the small sample size of only 3 patients. While these patients may not be representative of the larger population of individuals with urothelial cancer, our analysis of RNA-sequencing data from The Cancer Genome Atlas suggests that the average expression of PSMA is low across this malignancy.

In conclusion, PSMA-targeted ^{18}F-DCFPyL PET/CT is likely of limited clinical value for imaging patients with urothelial carcinoma. This can be explained by low levels of target PSMA expression within the tumor neovasculature. Future research efforts should focus on the development of other molecularly targeted imaging agents for this disease.

Acknowledgments

Sources of Funding: National Institutes of Health grants CA134675 and CA183031

References

1. Clark PE, Agarwal N, Biagioli MC, et al. Bladder cancer. J Natl Compr Canc Netw. 2013; 11(4): 446–75. [PubMed: 23584347]

2. Mertens LS, Meijer RP, Meinhardt W, et al. Occult lymph node metastases in patients with carcinoma invading bladder muscle: incidence after neoadjuvant chemotherapy and cystectomy vs after cystectomy alone. BJU Int. 2014; 114(1):67–74. [PubMed: 24053889]

3. Zhang H, Xing W, Kang Q, Chen C, Wang L, Lu J. Diagnostic value of [18F] FDG-PET and PET/CT in urinary bladder cancer: a meta-analysis. Tumour Biol. 2015; 36(5):3209–14. [PubMed: 25809703]

4. Soubra A, Hayward D, Dahm P. The diagnostic accuracy of ^{18}F-fluorodeoxyglucose positron emission tomography and computed tomography in staging bladder cancer: a single-institution study and a systematic review with meta-analysis. World J Urol. 2016; 34(9):1229–37. [PubMed: 26847182]

5. Pichler R, De Zordo T, Fritz J, et al. Pelvic lymph node staging by combined ^{18}F-FDG-PET/CT imaging in bladder cancer prior to radical cystectomy. Clin Genitourin Cancer. 2017; 15(3):e387–e395. [PubMed: 27601364]

6. Vind-Kezunovic S, Bouchelouche K, Ipsen P, Høyer S, Bell C, Bjerggaard Jensen J. Detection of lymph node metastasis in patients with bladder cancer using maximum standardised uptake value and ^{18}F-fluorodeoxyglucose positron emission tomography/computed tomography: results from a high-volume centre including long-term follow-up. Eur Urol Focus. 2017 in press.

7. Chang SS, O'Keefe DS, Bacich DJ, Reuter VE, Heston WD, Gaudin PB. Prostate-specific membrane antigen is produced in tumor-associated neovasculature. Clin Cancer Res. 1999; 5(10): 2674–81. [PubMed: 10537328]

8. Chang SS, Reuter VE, Heston WD, Bander NH, Grauer LS, Gaudin PB. Five different anti-prostate-specific membrane antigen (PSMA) antibodies confirm PSMA expression in tumor-associated neovasculature. Cancer Res. 1999; 59(13):3192–8. [PubMed: 10397265]

9. Baccala A, Sercia L, Li J, Heston W, Zhou M. Expression of prostate-specific membrane antigen in tumor-associated neovasculature of renal neoplasms. Urology. 2007; 70(2):385–90. [PubMed: 17826525]

10. Gala JL, Loric S, Guiot Y, et al. Expression of prostate-specific membrane antigen in transitional cell carcinoma of the bladder: prognostic value? Clin Cancer Res. 2000; 6(10):4049–54. [PubMed: 11051255]

11. Maurer T, Eiber M, Schwaiger M, Gschwend JE. Current use of PSMA-PET in prostate cancer management. Nat Rev Urol. 2016; 13(4):226–35. [PubMed: 26902337]

12. Rowe SP, Gorin MA, Hammers HJ, et al. Imaging of metastatic clear cell renal cell carcinoma with PSMA-targeted ^{18}F-DCFPyL PET/CT. Ann Nucl Med. 2015; 29(10):877–82. [PubMed: 26286635]

13. Rowe SP, Gorin MA, Hammers HJ, Pomper MG, Allaf ME, Javadi MS. Detection of ^{18}F-FDG PET/CT occult lesions with ^{18}F-DCFPyL PET/CT in a patient with metastatic renal cell carcinoma. Clin Nucl Med. 2016; 41(1):83–5. [PubMed: 26402128]

14. Rhee H, Blazak J, Tham CM, et al. Pilot study: use of gallium-68 PSMA PET for detection of metastatic lesions in patients with renal tumour. EJNMMI Res. 2016; 6(1):76. [PubMed: 27771904]

15. Gorin MA, Rowe SP, Hooper JE, et al. PSMA-Targeted ^{18}F-DCFPyL PET/CT imaging of clear cell renal cell carcinoma: results from a rapid autopsy. Eur Urol. 2017; 71(1):145–146. [PubMed: 27363386]

16. Sawicki LM, Buchbender C, Boos J, et al. Diagnostic potential of PET/CT using a ^{68}Ga-labelled prostate-specific membrane antigen ligand in whole-body staging of renal cell carcinoma: initial experience. Eur J Nucl Med Mol Imaging. 2017; 44(1):102–107. [PubMed: 26996777]

17. Sasikumar A, Joy A, Pillai MRA, Alex TM, Narayanan G. ^{68}Ga-PSMA PET/CT in osteosarcoma in fibrous dysplasia. Clin Nucl Med. 2017; 42(6):446–447. [PubMed: 28346248]

18. Sasikumar A, Joy A, Pillai MR, et al. Diagnostic value of ^{68}Ga-PSMA-11 PET/CT imaging of brain tumors-preliminary analysis. Clin Nucl Med. 2017; 42(1):e41–e48. [PubMed: 27846000]

19. Sathekge M, Lengana T, Modiselle M, et al. ^{68}Ga-PSMA-HBED-CC PET imaging in breast carcinoma patients. Eur J Nucl Med Mol Imaging. 2017; 44(4):689–694. [PubMed: 27822700]

20. Sasikumar A, Joy A, Pillai M, Bindu S, Sudin SR. ^{68}Ga-PSMA uptake in an incidentally detected gastrointestinal stromal tumor in a case of suspected carcinoma prostate. Clin Nucl Med. 2017; 42(10):e447–e448. [PubMed: 28759526]
21. Sasikumar A, Joy A, Nanabala R, Pillai MR, Thomas B, Vikraman KR. ^{68}Ga-PSMA PET/CT imaging in primary hepatocellular carcinoma. Eur J Nucl Med Mol Imaging. 2016; 43(4):795–6. [PubMed: 26743897]
22. Verburg FA, Krohn T, Heinzel A, Mottaghy FM, Behrendt FF. First evidence of PSMA expression in differentiated thyroid cancer using [^{68}Ga]PSMA-HBED-CC PET/CT. Eur J Nucl Med Mol Imaging. 2015; 42(10):1622–3. [PubMed: 25916744]
23. Pandit-Taskar N, O'Donoghue JA, Divgi CR, et al. Indium 111-labeled J591 anti-PSMA antibody for vascular targeted imaging in progressive solid tumors. EJNMMI Res. 2015; 5:28. [PubMed: 25984435]
24. Milowsky MI, Nanus DM, Kostakoglu L, et al. Vascular targeted therapy with anti-prostate-specific membrane antigen monoclonal antibody J591 in advanced solid tumors. J Clin Oncol. 2007; 25(5):540–7. [PubMed: 17290063]
25. Gupta M, Choudhury PS, Gupta G, Gandhi J. Metastasis in urothelial carcinoma mimicking prostate cancer metastasis in Ga-68 prostate-specific membrane antigen positron emission tomography-computed tomography in a case of synchronous malignancy. Indian J Nucl Med. 2016; 31(3):222–4. [PubMed: 27385897]
26. Szabo Z, Mena E, Rowe SP, et al. Initial evaluation of [^{18}F]DCFPyL for prostate-specific membrane antigen (PSMA)-targeted PET imaging of prostate cancer. Mol Imaging Biol. 2015; 17(4):565–74. [PubMed: 25896814]
27. Rowe SP, Drzezga A, Neumaier B, et al. Prostate-specific membrane antigen-targeted radiohalogenated PET and therapeutic agents for prostate cancer. J Nucl Med. 2016; 57(suppl 3): 90S–96S. [PubMed: 27694179]
28. Rowe SP, Gorin MA, Salas Fragomeni RA, Drzezga A, Pomper MG. Clinical experience with ^{18}F-labeled small molecule inhibitors of prostate-specific membrane antigen. PET Clin. 2017; 12(2): 235–241. [PubMed: 28267456]
29. Dietlein M, Kobe C, Kuhnert G, et al. Comparison of [^{18}F]DCFPyL and [^{68}Ga]PSMA-HBED-CC for PSMA-PET imaging in patients with relapsed prostate cancer. Mol Imaging Biol. 2015; 17(4): 575–84. [PubMed: 26013479]
30. Dietlein F, Kobe C, Neubauer S, et al. PSA-stratified performance of ^{18}F- and ^{68}Ga-PSMA PET in patients with biochemical recurrence of prostate cancer. J Nucl Med. 2017; 58(6):947–952. [PubMed: 27908968]
31. Li B, Dewey CN. RSEM: accurate transcript quantification from RNA-seq data with or without a reference genome. BMC Bioinformatics. 2011; 12:323. [PubMed: 21816040]
32. Wang K, Singh D, Zeng Z, et al. MapSplice: accurate mapping of RNA-seq reads for splice junction discovery. Nucleic Acids Res. 2010; 38(18):e178. [PubMed: 20802226]

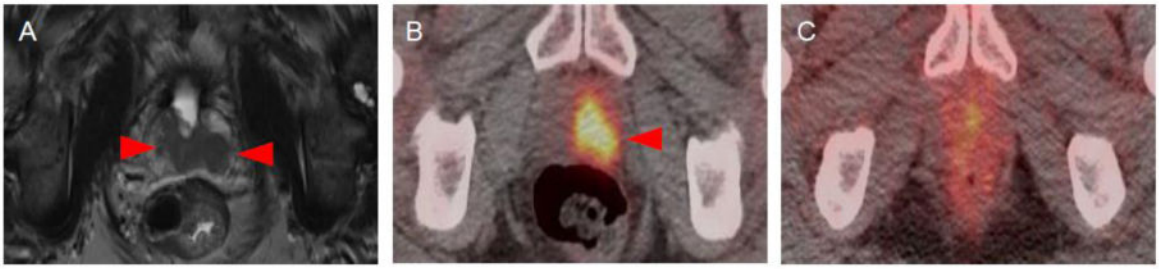

Figure 1.

Imaging findings of Patient 1. (A) T2-weighted MRI image demonstrating recurrent urothelial carcinoma of the prostatic urethra (red arrows). (B) The lesion had a high degree of radiotracer uptake on ^{18}F-FDG PET/CT SUV_{max} = 9.0, red arrow) (C) but had no discernable uptake above background on ^{18}F-DCFPyL PET/CT.

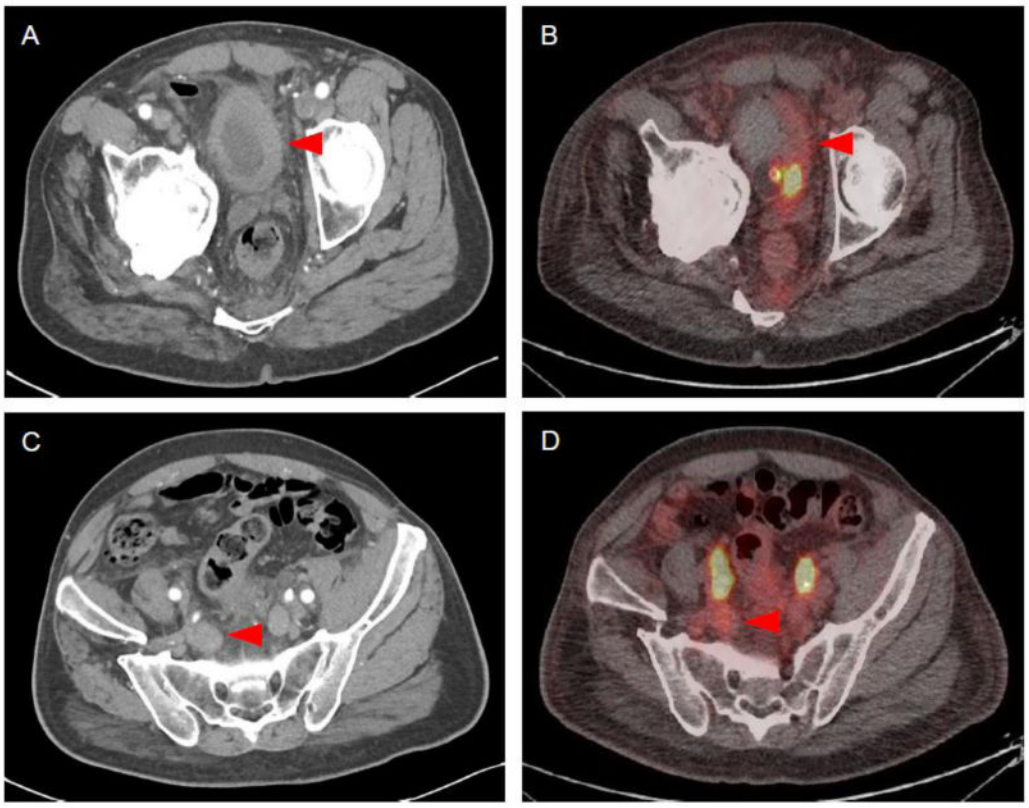

Figure 2.

Imaging findings of Patient 2. (A) Contrast-enhanced CT demonstrated a primary tumor of the bladder. (B) This lesion had only modest radiotracer uptake on ^{18}F-DCFPyL PET/CT (SUV_{max} = 2-2.5). (C) Contrast-enhanced CT also demonstrated pelvic lymph node involvement. (D) This lesion was poorly localized on ^{18}F-DCFPyL PET/CT (SUV_{max} = 2.0-2.5).

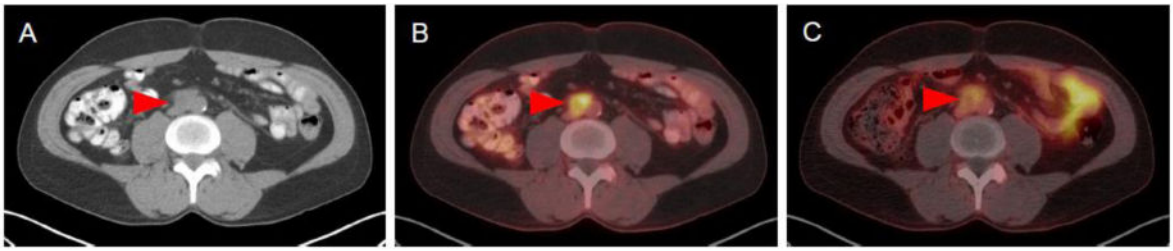

Figure 3.

Imaging findings of Patient 3. (A) The patient had a 2.2 cm retroperitoneal portocaval lymph node on contrast-enhanced CT. (B) This lesions was avid for ^{18}F-FDG (SUV_{max} = 5.7) and (C) to a lesser extent ^{18}F-DCFPyL (SUV_{max} = 3.1).

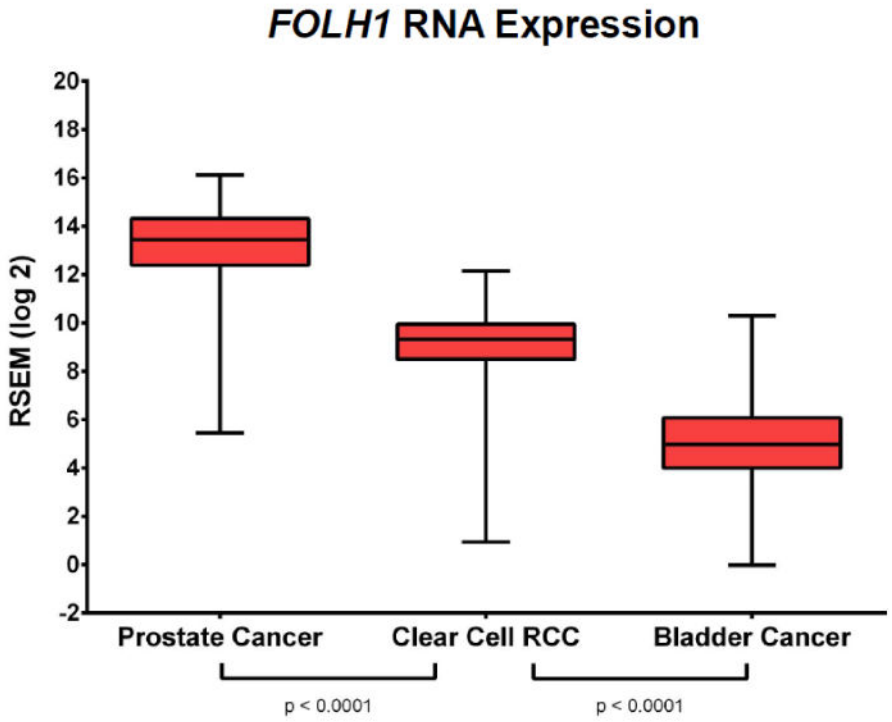

Figure 4.

Comparison of *FOLH1* RNA expressions levels among cases of prostate cancer, clear cell renal cell carcinoma, and bladder cancer from The Cancer Genome Atlas. Of these malignancies, urothelial carcinoma of the bladder had the lowest level of *FOLH1* expression.

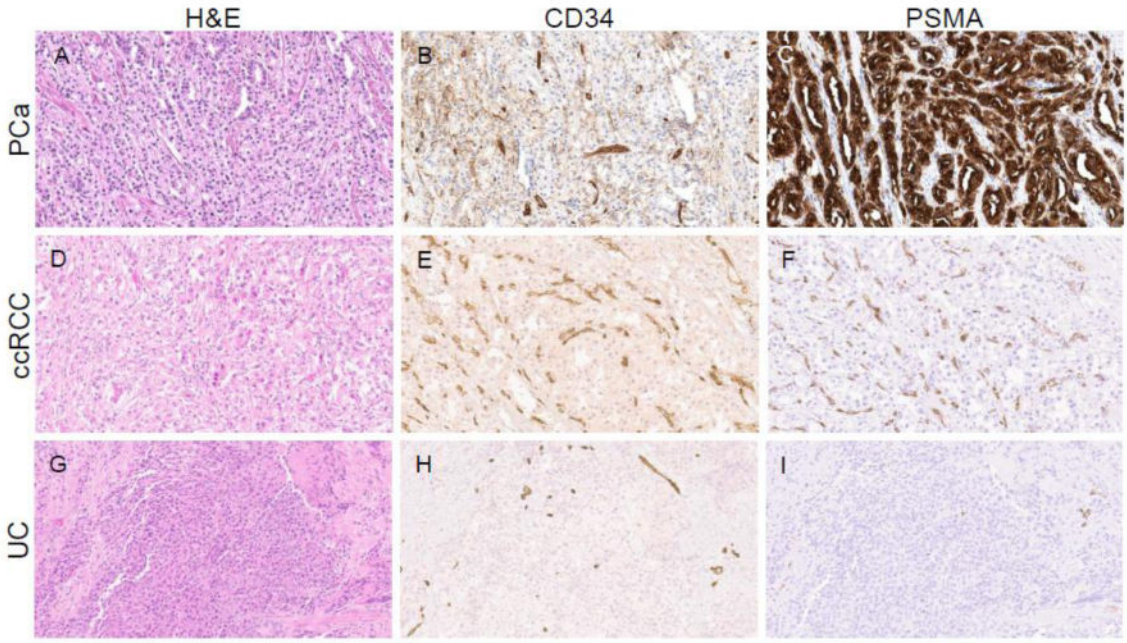

Figure 5.

Comparison of PSMA protein expression in a case of prostate cancer (PCa), clear cell RCC (ccRCC), and urothelial carcinoma of the bladder (UC). (A, D, G) Hematoxylin and eosin (H&E), and immunohistochemical staining for (B, E, H) the endothelial marker CD34 and (C, F, I) PSMA. (A-C) The case of prostate cancer had abundant expression of PSMA on the tumor epithelial cells (D-F) whereas the case of ccRCC demonstrated PSMA expression on endothelial cells within the neovasculature. (G-I) The case of UC had scant neovascularization and almost no detectable PSMA staining.

Table 1

Characteristics of imaged patients with metastatic urothelial carcinoma

Patient #	Age (years)	Sex	Primary Tumor Site	Race	Treatment Prior to Imaging	Sites of Disease on Conventional Imaging
1	66	Male	Bladder	White	Gemcitabine/cisplatin followed by atezolizumab	Prostatic urethra
2	67	Male	Bladder	Black	None	Bladder and pelvic lymph nodes
3	54	Male	Right Renal Pelvis	White	Right nephrouretherectomy followed by gemcitabine/cisplatin	Retroperitoneal lymph nodes and lung